

Hybrid Control for Biped Robots Using Impedance Control and Computed-Torque Control

Jong Hyeon Park and Hoam Chung

School of Mechanical Engineering
Hanyang University
Seoul, 144-791, Korea
email: jongpark@email.hanyang.ac.kr

Abstract

This paper proposes a hybrid control method of using the impedance control and the computed-torque control for biped robot locomotion. The computed-torque control is used for supporting (constrained) leg. For the free leg, the impedance control is used, where different values of impedance parameters are used depending on the gait phase of the biped robot. To reduce the magnitude of an impact and guarantee a stable footing when a foot contacts with the ground, this paper proposes to increase the damping of the leg drastically and to modify the reference trajectory of the leg. Computer simulations with a 3-dof environment model for which a combination of a nonlinear and a linear compliant contact models is used, show that the proposed controller is superior to the computed-torque controllers in reducing impacts and stabilizing the footing.

1 Introduction

Implementations of biped robots that have high mobility in a tight living space of the human are a key to bringing more robots closer to the human. Currently, more researchers in many countries are working on biped robots than ever before.

Many different control laws for biped robots are proposed such as the computed-torque controller [7], and the hybrid position/force controller [2]. While tracking the desired trajectory of the legs, a good biped robot controller should manage a stable contact of the swinging leg with the ground in its landing phase. Bouncing of the foot off the ground could cause instability in the locomotion.

In this paper, a hybrid control with impedance con-

trol and computed-torque control is proposed to deal with ground contacts of the swinging leg. Computed-torque control method is used for the supporting leg and the impedance control is used for the swinging leg. In typical human locomotion, leg muscles are repeatedly hardened and relaxed depending on the gait phase and result in very soft contacts with the ground. Using the same idea, the parameters of the impedance control are modulated depending on its gait phase in order to have stable contacts.

To simulate locomotion of a biped robot, its environment also should be modeled. In this paper, a 3-dof environment model using a combination of the nonlinear compliant contact model [5] and the linear compliant model [6] is used. This model can simulate small movements of the feet due to shock-absorbing pads underneath them and provides realistic reaction forces, unlike some plastic collision models such as [1].

The dynamics of the biped robot and a 3-dof environment model are described in Section 2. Design of the impedance controller and the impedance modulation strategy are presented in Section 3. Section 4 describes computer simulations, followed by conclusions in Section 5.

2 Environment Model and Dynamics of Biped Robot

2.1 3-DOF Environment Model

The impact force can be very large when the foot of the freely swinging leg contacts with the ground. In order to control such impacts actively, robots should have controllers with very high bandwidth and actuators with significantly large power. Instead, many biped robots are equipped with some kinds of shock-

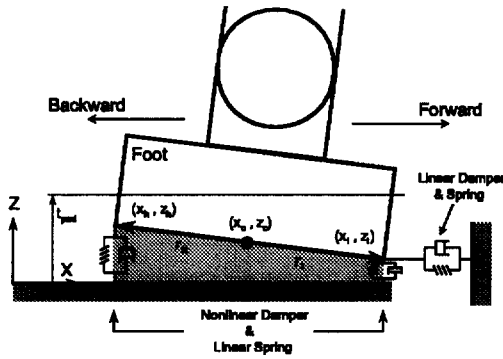


Figure 1: A 3-dof environment model

absorbing pads under their feet to avoid such large impacts. Such pads, in turn, allow small movements of the feet, and might cause unstable locomotion. In this paper, locomotion of biped robots with pads underneath their feet is considered. For simulation, pads are modeled as compliant contact models with linear springs and linear and nonlinear dampers. A nonlinear damper model is used in the vertical direction as [5] while a linear damper model is used in the horizontal direction, i.e., along the ground. The reaction force generated by the pad is thus

$$f = -\frac{3}{2}\alpha k p \dot{p} - k p \quad (1)$$

where p is the penetration depth, k is the pad stiffness, and α is a constant that defines the relation between the coefficient of restitution and the impact velocity.

Figure 1 describes a foot of the biped robot with a pad along with its environment, the ground. In the figure, (x_c, z_c) , (x_h, z_h) , and (x_t, z_t) denote the positions of the center of the sole, the heel and the toe of the foot, respectively; r_h and r_t denote vectors from (x_c, z_c) to (x_h, z_h) , and from (x_c, z_c) to (x_t, z_t) , respectively; and t_{pad} denotes the thickness of the undeformed foot pad. Two sets of a nonlinear damper and a linear spring are located at the tip and heel of the foot to depict the pad effect in the vertical direction. A single set of a linear damper and spring model is located at the tip to handle the pad effect along the ground.

Thus, vertical force f_v applied to the foot consists of the vertical forces at the heel and the toe, $f_{v,h}$ and

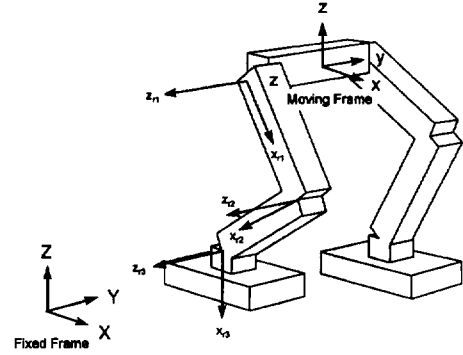


Figure 2: Coordinate frames of the biped robot

$f_{v,t}$, respectively, which are

$$f_{v,i} = \begin{cases} -\frac{3}{2}\alpha k_v(t_{pad} - z_i)\dot{z}_i - k_v(t_{pad} - z_i) & z_i < t_{pad} \\ 0 & z_i \geq t_{pad} \end{cases}$$

where $i = h$ for the heel, and $i = t$ for the tip.

$$f_v = f_{v,h} + f_{v,t} \quad (2)$$

For horizontal force f_h ,

$$f_h = -b_h \dot{x}_{ue} - k_h(x_{ue} - x_{org})$$

where x_{org} is the horizontal datum of the foot position to compute the horizontal elastic force, and is defined to be the position of the foot at the moment of its initial contact with the ground. Assuming that the angle of the foot against the ground is negligible, we can neglect the moment due to the horizontal force. Thus, the moment m_c exerted at (x_c, z_c) is computed by

$$m_c = r_h \times f_{v,h} + r_t \times f_{v,t}. \quad (3)$$

2.2 Dynamics of Biped Robot

The biped robot used in the paper is shown in Fig. 2. It has 3 degrees of freedom at each leg. Thus, its motions only in the sagittal plane are to be considered.

Biped robots are different from the typical manipulators in that they have no fixed contact points with the ground, and the constraints between the feet and the ground change repeatedly as they walk. The dynamics of the biped robot used in the paper is described by

$$H_c \ddot{q}_c + G_c a_0 + D_c \dot{h}_c + n_c = \tau_c, \quad (4)$$

$$H_u \ddot{q}_u + G_u a_0 + n_u = \tau_u, \quad (5)$$

$$Q_c \ddot{q}_c + Q_u \ddot{q}_u + R a_0 + P_c \dot{h}_c + g = 0, \quad (6)$$

where $\ddot{q} \in \mathbb{R}^6$, $a_0 \in \mathbb{R}^6$, and $h \in \mathbb{R}^6$ are the joint acceleration, acceleration of the base link, and constrained force, respectively; $H, G, D \in \mathbb{R}^{6 \times 6}$ are inertia matrix of the legs, the matrix denoting the dynamic effects of the base link to each link chain, and a Jacobian matrix, respectively; $L \in \mathbb{R}^6$, $Q, P, R \in \mathbb{R}^{6 \times 6}$, and $g \in \mathbb{R}^6$ are Coriolis and centripetal term, gravitational effects, the matrix denoting the dynamic effects of the link chains to the base link, the matrix denoting the dynamic effects of the constrained force to the base link, the inertia matrix of the base link, and a term including the gravitational effects of the base link.

Equations (4) and (5) describe the dynamics of the supporting (or constrained) leg and the free swinging (or unconstrained) leg, respectively; and Eq. (6) describes the dynamics of the base link coupled with the leg motions. Subscripts 'c' and 'u' denote 'constrained' and 'unconstrained', respectively.

3 Hybrid Control of Biped Robot

The control law is derived under the assumption that there exist contact sensors and force sensors at the robot feet and that the controller knows when a foot is in contact with the ground.

3.1 Gait Phases and Control Strategy

Borrowing some of the concept on the gait of normal human walking from an orthopedic research [9], we divided a gait cycle into three phases depending on the load exerted at the leg: swing phase, weight acceptance phase, and single support phase. A leg moves freely in the space in its swing phase. The weight acceptance phase of a leg begins when it hits the ground and ends when the other leg starts its swing phase. During the weight acceptance phase, the leg should absorb the initial impact energy and then incrementally accept the robot weight. The single support phase begins at the end of the weight acceptance phase, during which the leg supports the most of the robot weight and generates the torque to move the base link forward.

This paper proposes to use a different control scheme for each leg depending on its motion phase. First, during the swing phase and the weight acceptance phase, the impedance control law is applied. The only difference in them is that higher damping ratio is used in the latter phase in order to absorb the impact energy. During the single support phase, the computed-torque control law is used for precise tracking of the base link.

3.2 Impedance Control for Unconstrained Leg

From the relationship between the joint angular velocity, \dot{q} , and the foot velocity of the unconstrained leg, $\dot{x}_{ue} \in \mathbb{R}^6$,

$$\dot{x}_{ue} = v_0 + J_{ue}\dot{q}_u \quad (7)$$

where $v_0 \in \mathbb{R}^6$ is the velocity of the base link. Differentiating Eq. (7) results in

$$\ddot{x}_{ue} = a_0 + \dot{J}_{ue}\dot{q}_u + J_{ue}\ddot{q}_u$$

or

$$\ddot{q}_u = J_{ue}^{-1}(\ddot{x}_{ue} - a_0 - \dot{J}_{ue}\dot{q}_u) \quad (8)$$

Substituting this equation into Eq. (5) results in

$$\tau_u = H_u J_{ue}^{-1}(\ddot{x}_{ue} - a_0 - \dot{J}_{ue}\dot{q}_u) + G_u a_0 + n_u. \quad (9)$$

Suppose that the desired impedance of the foot of the unconstrained leg is

$$M_u(\ddot{x}_{ue} - \ddot{x}_{ue,d}) + B_u(\dot{x}_{ue} - \dot{x}_{ue,d}) + K_u(x_{ue} - x_{ue,d}) = f_0 - f, \quad (10)$$

where subscript 'd' denotes the desired value, M_u , B_u , and K_u are the desired mass, damping ratio, and stiffness; and f is the resultant external force. Due to the effect of the pad stiffness, reference force f_0 is expressed as

$$f_0 = \begin{cases} \begin{bmatrix} 0_{2 \times 1} \\ K_u t_{pad} \\ 0_{3 \times 1} \end{bmatrix} & \text{if the pad is squeezed,} \\ 0_{6 \times 1} & \text{otherwise} \end{cases}$$

In order to achieve the desired impedance of Eq. (10), acceleration \ddot{x}_{ue} should be

$$\ddot{x}_{ue} = \ddot{x}_{ue,d} - M_u^{-1}B_u(\dot{x}_{ue} - \dot{x}_{ue,d}) - M_u^{-1}K_u(x_{ue} - x_{ue,d}) + M_u^{-1}(f_0 - f), \quad (11)$$

Assuming $\ddot{x}_{ue,d} = 0$, and substituting Eq. (11) into Eq. (9) results in

$$\tau_u = H_u J_{ue}^{-1}[-M_u^{-1}B_u(\dot{x}_{ue} - \dot{x}_{ue,d}) - M_u^{-1}K_u(x_{ue} - x_{ue,d}) + M_u^{-1}(f_0 - f) - a_0 - \dot{J}_{ue}\dot{q}_u] + G_u a_0 + n_u, \quad (12)$$

which is the joint torque for the unconstrained leg.

3.3 Impedance Modulation

During the swing phase and weight acceptance phase, the leg experiences a transition from a free space motion to a constrained motion. While a relatively good tracking performance is required in the swing phase, and behaviors for the impact regulation and weight acceptance are needed from the moment of an impact to just before the single support phase. Especially, at the moment of impact, the impact shock should be absorbed and the bouncing of the foot must be suppressed.

At the moment of the contact, the control law increases the damping ratio of the desired impedance of the foot 50 times its critical value. The stiffness and mass components in the impedance model is selected to match the desired stiffness and the cutoff frequency of the controller, which is similar to the method used in [10]. This method of increasing the damping ratio at the moment of impact is very simple but highly effective to regulate the impact transition.

To enhance further its capability in its impact regulation, the controller sets the reference vertical position and velocity to zero right after an initial contact of the foot with the ground is detected, regardless of the reference trajectory of the foot.

3.4 Computed-Torque Control for Constrained Leg

The joint torque, τ_c for the constrained (supporting) leg is computed using the computed-torque control method. The computed-torque control law with respect to the base link can be derived similarly to the method used in [7].

From Eq. (5) and Eq. (4),

$$\ddot{q}_c = H_c^{-1}(\tau_c - G_c a_0 - D_c h_c - n_c), \quad (13)$$

$$\ddot{q}_u = H_u^{-1}(\tau_u - G_u a_0 - n_u). \quad (14)$$

Substituting Eqs. (13) and (14) into Eq. (6) results in

$$Q_c H_c^{-1} \tau_c - \tilde{R} a_0 + \tilde{P} h_c + \tilde{g} = 0, \quad (15)$$

where

$$\begin{aligned} \tilde{R} &= Q_c H_c^{-1} G_c + Q_u H_u^{-1} G_u - R, \\ \tilde{g} &= g + Q_u H_u^{-1} (\tau_u - n_u) - Q_c H_c^{-1} n_c, \\ \tilde{P} &= P_c - Q_c H_u^{-1} D_c. \end{aligned}$$

From this,

$$\tau_c = (Q_c H_c^{-1})^{-1} \{ \tilde{R} a_0 - \tilde{P} h_c - \tilde{g} \}. \quad (16)$$

If joint torque for the constrained leg is selected as

$$\tau_c = (Q_c H_c^{-1})^{-1} \{ \tilde{R} (a_{0,d} - u_c) + \tilde{P} h_c - \tilde{g} \}, \quad (17)$$

where

$$u_c = -K_v \dot{e}_0 - K_p e_0,$$

and e_0 is the position error of the base link, i.e.,

$$e_0 = x_{0,d} - x_0,$$

then, from Eqs. (17) and (16), the error dynamics of the base link becomes

$$\ddot{e}_0 + K_v \dot{e}_0 + K_p e_0 = 0. \quad (18)$$

Therefore, e_0 is asymptotically stable only if $K_v, K_p > 0$.

4 Simulations

The effectiveness of the hybrid control with impedance modulation is to be shown in computer simulations. The robot parameters for the simulations is summarized in Table 1. The parameters of the environment model used in the simulations are shown in Table 2. The pads underneath the feet are 1 cm thick.

In the first simulation, the proposed control algorithm is applied to the biped robot under the assumption that there's no uncertainty in the robot parameters and the ground geometry. Initially, the robot stands still with its feet on the ground. Then, the left leg is lifted first and the base link starts moving forward along the desired trajectory, which is based on the locomotion at 0.1 m in 0.4s. When the left leg comes into a contact with the ground, it moves into the weight acceptance phase for 0.1 s.

From the second gait, the robot walks steadily and its gait parameters such as the stance, maximum height of foot and the period of gait become as twice as those in the first gait. Figure 3 shows the vertical motions of the feet. Figure 4 shows foot motions during the weight acceptance phase in more details. From this, it can be observed that the right foot does not bounce off the ground at the initial impact and increasingly takes more weight of the robot.

For comparisons, the same simulation but with only the computed-torque control method through out all the gait phases is done. Its results are shown in Fig. 5. Note that the right foot bounces off the ground initially, and the entire supporting state becomes unstable.

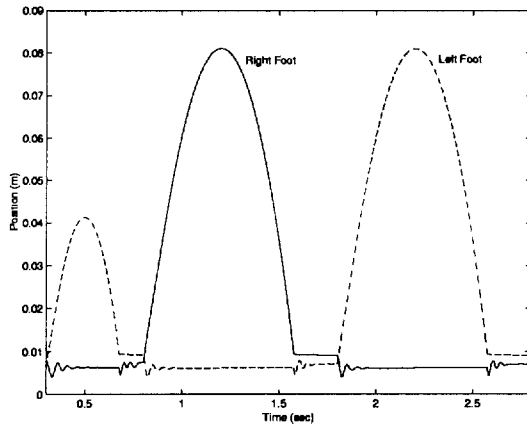


Figure 3: Walking with the hybrid control

Table 1: Parameters of the biped robot

link	link length (m)	link mass (kg)
1	0.3	1
2	0.3	1
3	0.1	1
base	0.3	10

The performance of the computed-torque algorithm can be significantly deteriorated with model uncertainties, which may result in unstable biped locomotion. Thus, in the second simulation, it is assumed that the exact values of robot parameters are not available. Even when the estimation errors on the robot inertias are as high as $\pm 40\%$, no significant deviations from the first simulation were observed. Figure 6 shows that a very small deviation in the elevation of the base link. Deviations of other variables including the horizontal position of base link are negligibly small. And, more importantly, the locomotion remains stable.

According to [4], a small deviation of the ground level can cause the destabilization of the entire walking with position control only. In the third simulation, response to the uncertainty in the ground level is simulated. At the second gait, the robot encounters the ground level that is 1 cm higher than the previous gait. Figure 7 shows that the excellent adaptability of the proposed controller to an uneven ground surface, without any other costly on-line adaptation schemes.

The results of the simulations show that the proposed hybrid controller regulates impact shocks and contacts with the ground very well and robustly.

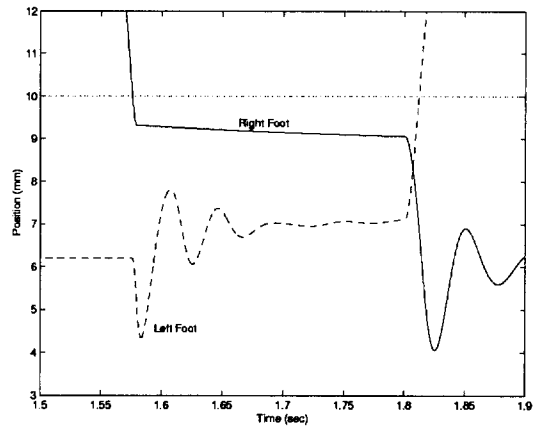


Figure 4: Closer view on the impact with the impedance control during the weight acceptance phase

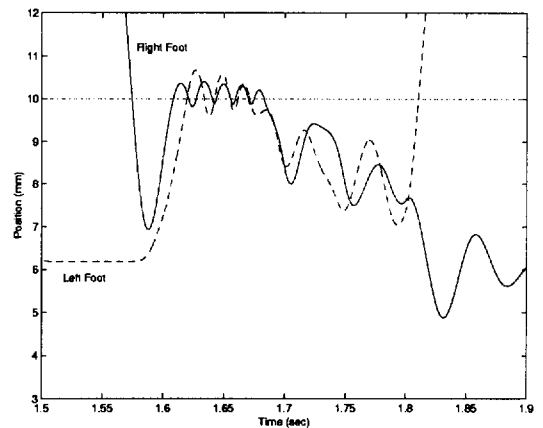


Figure 5: Unstable footing resulted during the weight acceptance phase with the computed-torque control method.

5 Conclusions

A hybrid controller using the impedance control and the computed-torque control is proposed to control biped robots which repeatedly interact with the external environment. To investigate the performance of the proposed controller, biped robot locomotion is simulated with a 3-dof environment model with compliant contact models. The performance of the proposed controller is compared with that of the computed-torque controller only. The robustness of the proposed controller is verified through the simulations with model uncertainties. Moreover, the biped robot with the proposed controller can walk on an uneven surface without any on-line adaptation. The

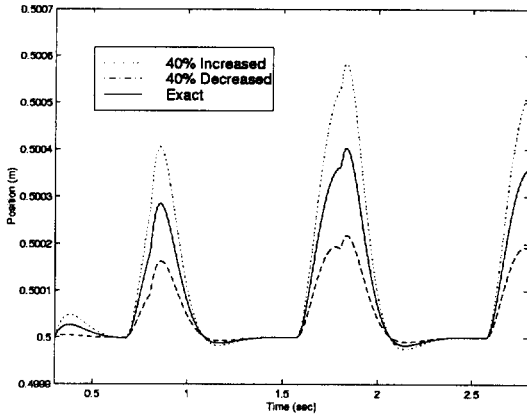


Figure 6: Elevation of the base link under the robot parameter uncertainties

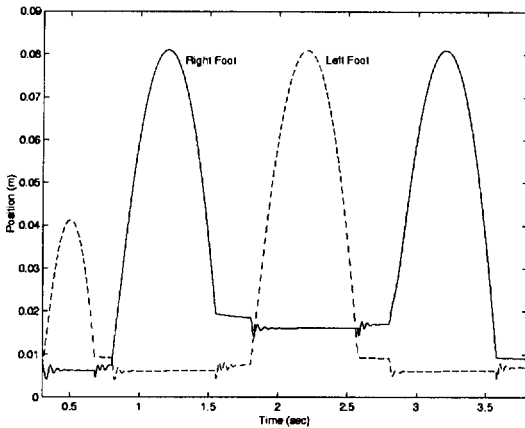


Figure 7: Walking on an uneven surface

simulation results shows that the proposed controller performs better than the computed-torque controller in stabilizing the robot footing.

Acknowledgement

This work is partially supported by the Korea Science and Engineering Foundation (KOSEF) under Project 986-1000-001-2.

References

[1] Y. Fujimoto and A. Kawamura, "Three Dimensional Digital Simulation and Autonomous Walk-

Table 2: Parameters of the foot pad model

α	0.5	k_v	2.0×10^4 N/m
k_h	1.5×10^5 N/m	b_h	1000 Ns/m

ing Control for Eight-Axis Biped Robot," Proc. Int. Conf. on Robotics and Automation, 1995.

[2] Y. Fujimoto and A. Kawamura, "Biped Walking Control with Optimal Foot Force Distribution by Quadratic Programming," Proc. of Advanced Intelligent Mechatronics, Tokyo, Japan, 1997.

[3] Y. Fujimoto and A. Kawamura, "Robust Control of Biped Walking Robot with Yaw Moment Compensation by Arm Motion," Proc. Asian Control Conference, Seoul, Korea, 1997.

[4] J. Yamaguchi, A. Takanishi, and I. Kato, "Experimental Development of a Foot Mechanism with Shock Absorbing Material for Acquisition of Landing Surface Position Information and Stabilization of Dynamic Biped Walking," Proc. Int. Conf. on Robotics and Automation, 1995.

[5] D. W. Marhefka and D. E. Orin, "Simulation of Contact Using a Nonlinear Damping Model," Proc. Int. Conf. on Robotics and Automation, 1996.

[6] P. R. Kraus and V. Kumar, "Compliant Contact Models for Rigid Body Collisions," Proc. Int. Conf. on Robotics and Automation, 1997.

[7] J. H. Park and K. D. Kim, "Biped Robot Walking Using Gravity-Compensated Inverted Pendulum Mode and computed Torque Control," Proc. Int. Conf. on Robotics and Automation, Leuven, Belgium, 1998.

[8] N. Hogan, "Impedance Control: An Approach to Manipulation Part I - III," J. of Dynamic Systems, Measurement, and Control, vol. 107, pp. 1-24, 1986.

[9] D. A. Winter, "Overall Principle of Lower Limb Support During Stance Phase of Gait," J. of Biomechanics, vol. 13, pp. 123-127, 1980.

[10] H. Kazerooni, T. B. Sheridan, and P. K. Houpt, "Robust Compliant Motion for Manipulators, Part I: The Fundamental Concepts of Compliant Motion," IEEE J. of Robotics and Automation, vol. 2, no.2, pp. 83-92, 1986.